

# Prediction of Relay Settings in an Adaptive Protection System

Adam Summers  
Electric Power System  
Research  
Sandia National  
Laboratories  
Albuquerque, NM, U.S.A  
asummer@sandia.gov

Trupal Patel  
Electric Power System  
Research  
Sandia National  
Laboratories  
Albuquerque, NM, U.S.A  
tpatel@sandia.gov

Ronald Mathews  
Electric Power System  
Research  
Sandia National  
Laboratories  
Albuquerque, NM, U.S.A  
rcmath@sandia.gov

Matthew J. Reno  
Electric Power System  
Research  
Sandia National  
Laboratories  
Albuquerque, NM, U.S.A  
mjreno@sandia.gov

**Abstract**—Communication-assisted adaptive protection can improve the speed and selectivity of the protection system. However, in the event that communication is disrupted to the relays from the centralized adaptive protection system, predicting the local relay protection settings is a viable alternative. This work evaluates the potential for machine learning to overcome these challenges by using the Prophet algorithm programmed into each relay to individually predict the time-dial (TDS) and pickup current ( $I_{PICKUP}$ ) settings. A modified IEEE 123 feeder was used to generate the data needed to train and test the Prophet algorithm to individually predict the TDS and  $I_{PICKUP}$  settings. The models were evaluated using the mean average percentage error (MAPE) and the root mean squared error (RMSE) as metrics. The results show that the algorithms could accurately predict  $I_{PICKUP}$  setting with an average MAPE accuracy of 99.961%, and the TDS setting with a average MAPE accuracy of 94.32% which is sufficient for protection parameter prediction.

**Index Terms**—prediction, prophet, adaptive protection, machine learning, relays

## I. INTRODUCTION

The future power system demands for a nearly uninterrupted power supply will put further strain on the protection system. Future protection schemes will have to respond with greater accuracy and precision for fault events, and system reconfigurations. Machine learning (ML) can provide advanced awareness of system conditions [1]. Relays can use a variety of protection schemes, such as distance, differential, and time-based methods to remove faults and maintain system stability [2]. Furthermore, unique system designs such as microgrids can introduce complicated protection schemes [3] that need to be updated depending on load, generation variability, and the system configuration.

As the penetration of inverter-based resources (IBRs) in the distribution and microgrids systems continue to increase, the protection scheme's selectivity, sensitivity, and reliability of the protection setting will have to change [4]. Adaptive protection has been purposed as a solution to handle the solar variability of IBRs in the power system. Different forms of adaptive

protection have been purposed to remedy the impacts that IBRs can have on a system, as mentioned previously. In [5], using a relay's multiple groups setting to store different protection parameters using a clustering algorithm is proposed. However, not all relays have the same number of groups, limiting the flexibility to have different types and costs of relays in a protection scheme. Communication with a centralized adaptive protection algorithm is a solution to the limited group settings that a relay can handle [6]. Local current and voltage measurements would be communicated, typically using SCADA, to a centralized adaptive protection algorithm that would use those measurements to calculate new protection settings. In [7], a sensitivity analysis is proposed to work with a centralized adaptive protection algorithm that would communicate settings to relays on an event-driven basis. However, communication-enabled protection systems can be problematic for several reasons.

First, if a single relay's line of communication in either direction is interrupted either unintentionally (weather-related, or equipment failure) or maliciously (cyber-attacks) for an extended period, the protection scheme may not operate with the speed and selectivity intended during that period. Secondly, if the main communication path to the adaptive protection algorithm is subjected to a loss of communication, then a complete miscoordination of the protection scheme is possible dependent upon the solar variability of the IBRs or configuration of the grid. Therefore, it will be advantageous to predict the protection settings locally for each relay if communication is disrupted.

Recent literature examined how machine learning (ML) algorithms could be used for forecasting and predicting loads and IBR generation [8],[9]. Many have explored predicting the present and future load demand [10],[11] on a system. System operators currently use IBR generation and load predictions to maintain system stability operations [12], with predictions on the hourly and day-ahead time horizon. This gives the power utility an idea about the future demand of consumers and an ample amount of time to mitigate the difference between generation capacity and load demand.

Herein, we propose using adaptive protection settings that are determined with [13] for the IEEE 123 feeder for year-long settings and working with the Prophet ML algorithm [14] to predict the time-overcurrent protection settings of individual relays.

While forecasting loads and IBR generation are well presented in the literature, predicting protection settings could not be identified. This paper will add to the previous work that used ML algorithms for power system forecasting by providing an analysis focused on the following items:

- Predicting a relay's local time dial setting (TDS) settings using the Prophet algorithm.
- Predicting a relay's local  $I_{PICKUP}$  settings using the Prophet algorithm.
- A review of the individual relay's predicted protection setting overall coordination.
- Using the local predicted protection settings to determine if settings communicated from the centralized adaptive protection algorithm have been compromised.

The IEEE 123 bus feeder was simulated in OpenDSS and generated the data that was used by the optimizer [13] to determine the time-over current directional setting used for predicting the relay's protection settings.

## II. SIMULATION DATA

### A. System of Study

The IEEE 123 feeder shown in Fig.1 was modeled in OpenDSS. A year-long, hourly simulation with varying residential and commercial loads and varying photovoltaic (PV) profiles were used. The feeder includes 10 relays. Four of them are used as tie lines for circuit reconfiguration. The methodology presented in Reimer et al [15] determined the relay locations based on the locations of the IBR. For the experiment, relay tie line one is open, and the other three tie lines are closed. Table I gives the IBR ratings and locations.

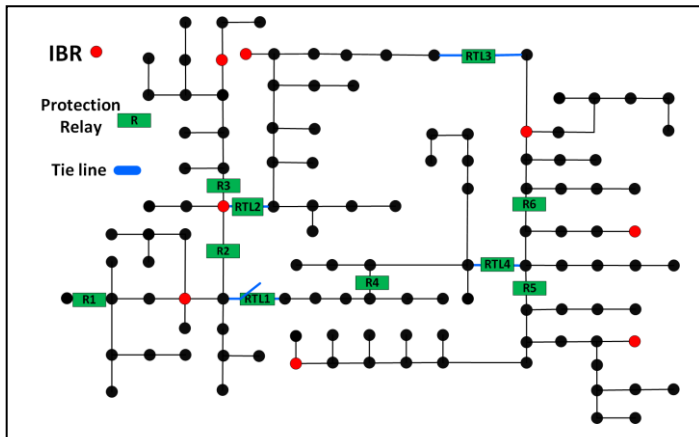


Figure 1. Modified IEEE 123 Feeder With DER and Relays.

TABLE I. IBR LOCATION AND RATING

Bus #	8	18	28	48	61	79	95	100	108
Inverter AC kVA Rating	500	700	500	1000	500	500	1000	500	500

### B. Procedure To Generate the Protection Data Set

The optimal protection coordination algorithm [13] generates relay settings by formulating the relay coordination problem as an MINLP problem which is solved and optimized using a genetic algorithm (GA) based solver. The optimal protection coordination algorithm works in conjunction with OpenDSS to obtain the network data to generate protection coordination pairs. Coordination pairs are determined by path tracing from source buses to load busses, identifying relays in the path to determine the relays that need to be coordinated. Fault analysis is then performed using OpenDSS to identify the fault currents observed by each protective device in the fault path. The fault currents along with the coordination pairs are used to write protection coordination constraints used as the constraint function for the solver. The protection coordination constraints ensure that there exist settings for the protection devices such that the primary device trips before its backup. The sum of the primary relay operating times is used as the objective function being minimized by the genetic algorithm. The objective function and the constraint function are used with the GA solver to find and optimize the relay settings. The final output of the optimizer would be Table II for each relay. The variables in Table II will be explained in Sec II-A.

TABLE II. EXAMPLE PROTECTION SETTING DATA

Date	TDS	$I_{PICKUP}$	OT
1/1/17 0:00	0.84	23.82	0.15
1/1/17 1:00	0.68	21.21	0.12

## III. PREDICTING AT SCALE

### A. The Prophet Algorithm

The Prophet algorithm, created by Taylor and Letham [14], models time series as a generalized additive model (GAM) represented by Eq 1.

$$y(t) = g(t) + s(t) + h(t) + \epsilon(t) \quad (1)$$

$g(t)$  represents the trend function that models the non-periodic changes in the value of the times,  $s(t)$  represents periodic changes, such as daily, weekly, and year seasonality,  $h(t)$  represents the effects of holidays which occur potentially at irregular schedules.  $\epsilon(t)$ , is an error term for any changes not accommodated by the model. Note that this model is inherently different from time series forecasting models, such as autoregressive forecasting, that predict the value at time  $t$  using measurements from  $t-1$ . Instead this formulation is essentially a curve-fitting exercise that provides advantages of not needing regularly spaced data, ability to handle missing data and outliers, and the ability to capture long seasonality trends. Each training point is a separate sample, where time is used as one of the regressors. The Prophet algorithm has several tunable hyperparameters. For a more in-depth discussion of the Prophet algorithm, the reader is referred to [14].

### B. Parameters to Predict

Eq 2 is the time overcurrent equation that the relays in this experiment will use. For this paper, we are interested in predicting the TDS and  $I_{\text{PICKUP}}$  from Eq 2 for each relay. The variables  $A$ ,  $B$ , and  $p$  relate to the curve type, which for each relay is set to an inverse (U2) type, and the variable  $I$  is the measured *rms* current on the secondary side of the relay. The variable OT is the final operating time of the relay. The TDS value can range from 0.25 to 15, while the  $I_{\text{PICKUP}}$  values range in the hundreds of amperes. In Table II, the columns in green indicate settings and operating time that the SNL Optimizer calculated from the local *rms* current and voltage relay measurements.

$$OT = TDS * \frac{A}{\left(\frac{I}{I_{\text{PICKUP}}}\right)^p} + B \quad (2)$$

### C. Model Calibration and Selection

All relays for this experiment had the same range of hyperparameters, user tunable parameters, that were explored to predict TDS and  $I_{\text{PICKUP}}$ . The mean average percentage error (MAPE) metric was used to evaluate and select each model for predicting the TDS and  $I_{\text{PICKUP}}$  settings and will be discussed in the next section. Figure 2 shows the data sets split between training and testing for relay 3 TDS. The training set contains data to the left of the vertical purple line. The test set is from the right of the vertical purple line. It is assumed that communications is lost at 11-23, so all model training must be performed before that point.

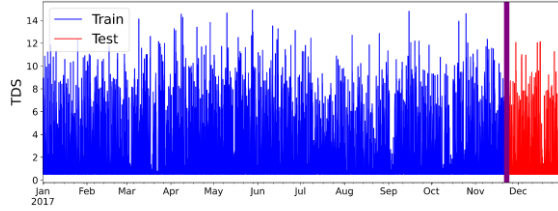


Figure 2. Relay 3 TDS Training and Test Splits

TABLE III. SELECTED MODEL PARAMETERS FOR TDS AND  $I_{\text{PICKUP}}$ . EACH RELAY NOTED IN FIGURE 1 IS A SEPARATE MODEL AS SHOWN BY EACH COLUMN.

	R1	R2	R3	R4	R5
Changepoint_prior_scale	TDS 0.4	0.5	0.3	0.3	0.5
	$I_{\text{PICKUP}}$ 0.5	0.3	0.3	0.2	0.1
Holidays_prior_scale	TDS 0.1	0.4	0.4	0.1	0.1
	$I_{\text{PICKUP}}$ 0.5	0.2	0.2	0.4	0.3
n_changepoints	TDS 200	100	100	100	100
	$I_{\text{PICKUP}}$ 100	100	100	100	100
Seasonality_mode	TDS M	A	A	A	A
	$I_{\text{PICKUP}}$ A	A	A	M	M
	R6	RTL2	RTL3	RTL4	
Changepoint_prior_scale	TDS 0.1	0.1	0.1	0.2	
	$I_{\text{PICKUP}}$ 0.3	0.4	0.3	0.4	
Holidays_prior_scale	TDS 0.5	0.5	0.3	0.4	
	$I_{\text{PICKUP}}$ 0.2	0.5	0.5	0.5	
n_changepoints	TDS 100	100	100	150	
	$I_{\text{PICKUP}}$ 100	150	100	150	
Seasonality_mode	TDS A	A	A	M	
	$I_{\text{PICKUP}}$ A	A	M	A	

Using the protection settings calculated and communicated to the individual relays from the optimizer [13], Sec II-B, and

local measurements, the TDS and  $I_{\text{PICKUP}}$  settings were predicted. Table III gives the final individual model parameters that were selected for predicting the TDS and the  $I_{\text{PICKUP}}$  protection parameter settings. The model with the lowest MAPE score was selected as the final model and will be discussed in Sec IV-B.

## IV. PREDICTION ANALYSIS

The predicting of the protection setting TDS and  $I_{\text{PICKUP}}$  focused on the potential of the Prophet algorithm's accuracy and precision. This prediction method considered the time-series dependencies of the data. Since the adaptive protection settings are dependant on the load in the feeder and the PV power output, the prediction method must incorporate the diurnal PV power shape as well as the seasonal and weekly load variations. This assessment used the data generated in Sec. II-B and the selected model in Sec. III to evaluate the individual relay models for predicting accuracy and precision. The simulation generated 8,360 data points for each relay. The first step involved splitting the dataset into a training set that contained 7,824 data points and a testing set that contained 936 data points. The final analysis used the testing data.

### A. Added Regressors

While the Prophet algorithm allows the direct forecasting of a variable of interest, it is often beneficial to include other features, known as regressors in the Prophet algorithm [14], to help build a prediction model. To determine which other regressors to include for predicting the TDS and  $I_{\text{PICKUP}}$  settings, individual correlation matrices for each relay were created from the generated data sets in Sec II-B. The regressors that were selected to add to the Prophet algorithm for the TDS relay models were: OT, and RMS phase-voltages. The regressors that were selected to add to the Prophet algorithm for the  $I_{\text{PICKUP}}$  relay models were the RMS phase-currents.

### B. Evaluation Metrics

The accuracy of the prediction was determined by how a model performed on new data (testing) that was not used when training the model. The TDS and  $I_{\text{PICKUP}}$  models with the lowest MAPE score were selected from Sec V. After the selected models were trained, the testing data was provided to the final model. The mean average percentage error (MAPE) and the root mean absolute error (RMSE) error metrics were used to evaluate the final models. MAPE is one of the most widely used metrics to check a prediction's accuracy. The RMSE is another widely used metric for assessing a predicting model's accuracy. Using these evaluation metrics provides a thorough review of each Prophet model's predicting abilities.

## V. RESULTS

Two different prediction models were made for each relay. The model that was designed to predict the TDS setting of each relay used the regressors OT, and the *rms* phase voltages, and the model that was designed to predict the  $I_{\text{PICKUP}}$  setting of each relay used the regressors *rms* phase currents. The added regressors were used to predict the same timestep for the TDS and  $I_{\text{PICKUP}}$  settings. The training set included the first 7,824 points of data indicated by values to the left of the purple vertical line in Fig 2. For the last part of the year, it is assumed that communication is lost, and the settings are predicted for

each time point using the trained Prophet algorithm with the time and other regressors (e.g. *rms* phase voltages) as inputs. In this scenario, it is assumed that each relay still has access to its local measurements like voltage and current to use as inputs to estimate the correct settings locally for that relay. Each model was evaluated on predicting the remaining 936 data points, the test set length, and compared to the actual values of that set. Table IV presents the final models MAPE and RMSE metric results for predicting and comparing to the testing data. The results only considered the prediction metrics for the test data set.

TABLE IV. MODEL EVALUATION METRICS RESULTS FOR EACH RELAY

	MAPE %		RMSE	
	TDS	I <sub>PICKUP</sub>	TDS	I <sub>PICKUP</sub>
<b>R1</b>	3.216	0.041	0.320	0.127
<b>R2</b>	8.038	0.004	0.721	0.013
<b>R3</b>	0.427	0.040	0.007	0.019
<b>R4</b>	0.469	0.021	0.005	0.005
<b>R5</b>	16.810	0.033	0.150	0.049
<b>R6</b>	12.459	0.034	0.505	0.064
<b>RTL2</b>	3.647	0.049	0.347	0.141
<b>RTL3</b>	5.290	0.031	0.410	0.057
<b>RTL4</b>	0.702	0.094	0.026	0.052

#### A. Predicting Results For TDS Settings

The MAPE metric for all but three relays were less than 5%. Relay's 2, 5, and 6 had the least good predictions for the TDS setting in Table IV. For example, relay 6 has a MAPE metric of 12.46% that signifies the average deviation from the actual TDS value that the optimizer [13] calculated over the testing period, from 2017-11-22 00:00:00 to 2017-12-31 23:00:00, that included 936-time points, was 84.54% accurate. However, the best prediction when using the MAPE metric was relay 3, which was 99.57 % accurate over the same period. Note that the MAPE for the TDS predictions was higher than the MAPE for the I<sub>PICKUP</sub>. This is partially due to the fact that the TDS are generally smaller numbers (less than 15), so the percent error metrics are higher than for I<sub>PICKUP</sub>.

The RMSE metric provides a different evaluation of the TDS prediction. Relay's 2, 6, and tie line 3 had the highest RMSE values. For example, relay 2 with the highest RMSE value of 0.721, means that on average the prediction values were 0.721 values away from the actual value. Fig 3 shows the predicted values plotted against the actual TDS setting for relay 2. The implication in the TDS predicted settings will be explored in the next section.

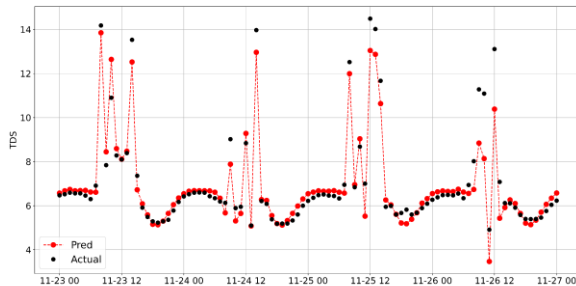


Figure 3. Relay 2 Comparison Between Predicted and Actual TDS Values.

#### B. Prediction Results For I<sub>PICKUP</sub> Settings

The MAPE metric for predicting the I<sub>PICKUP</sub> is significantly better than the prediction for TDS as shown in Table IV. For example, all relays have a MAPE metric well below 1%. This means that the prediction of I<sub>PICKUP</sub> for each relay was ~99.9% accurate with this metric. Figure 4 shows the prediction results for the I<sub>PICKUP</sub> setting for relay 6.

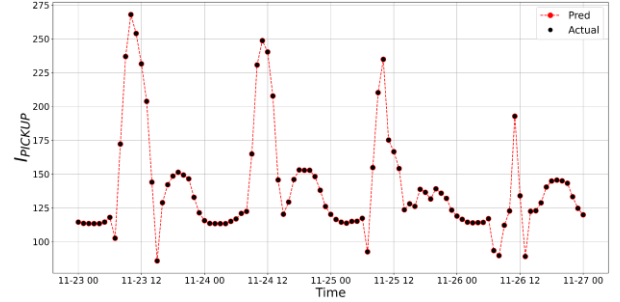


Figure 4. Relay 6 Comparison Between Predicted and Actual I<sub>PICKUP</sub> Values.

The RMSE metric provides a similar positive evaluation of the I<sub>PICKUP</sub> prediction. The I<sub>PICKUP</sub> setting for each relay is generally in the hundreds of amperes and the RMSE values for each prediction is in the tenths of amperes. Which for the I<sub>PICKUP</sub> setting in a relay would not affect the response of the relay.

#### C. A Review of The Coordination of Predicted Settings

If one or more relay's communication to the centralized adaptive protection algorithm is interrupted either unintentionally (weather-related, or equipment failure) or maliciously (cyber-attacks) for an extended period, the protection scheme may not operate with the speed and selectivity intended during that period. It is assumed that communication has been lost in Figure 5 and the predicted TDS values for relays 1, 2, 3, and tie line 2 are plotted.

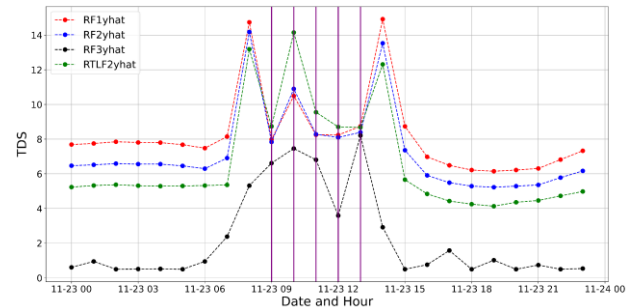


Figure 5. Relay Miscoordination Events

The vertical purple line represents events of TDS miscoordination for these relays. In Figure 5, there were 5 TDS miscoordination events. Overall there were 186 miscoordination events with the test set, which means coordination achieved an 80% accuracy for the TDS prediction.

#### D. Checking Adaptive Protection Algorithm Setting

The purposed Prophet algorithm can be used during a loss of communication as shown previously, and it could also be used to verify protection parameters that are communicated to

the relays. The Prophet algorithm produces an upper and lower prediction range. Figure 6 shows an example of using this upper and lower prediction range to detect and alert for an erroneous settings, such as the green star in the Figure 6 TDS value being sent to relay 2.

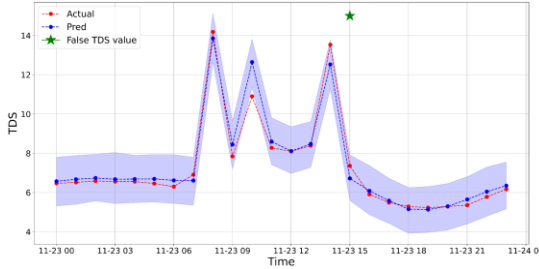


Figure 6. Relay 2 Using Upper and Lower Prediction Bounds To Detect An Erroneous TDS value.

## VI. CONCLUSIONS

The experiment found that using the Prophet algorithm to predict the TDS values, could achieve an average accuracy of 94.32% using the MAPE metric on the test data. The  $I_{PICKUP}$  prediction for each relay was able to achieve an average 99.961% accuracy on the test data. This proposed method can be extended to system reconfigurations and as new settings are determined by the optimizer the algorithm could be updated. This work provides a basis for future adaptive protection parameter prediction for individual relays either for the event of loss of communication or to verify settings communicated to the relays. This analysis could also be used to determine which relays have a substandard prediction and use that domain knowledge to add redundant communication paths to those relays.

## ACKNOWLEDGMENT

This material is based upon work supported by the U.S. Department of Energy's Office of Energy Efficiency and Renewable Energy (EERE) under the Solar Energy Technologies Office Award Number 36533. The paper describes objective technical results and analysis. Any subjective views or opinions that might be expressed in the paper do not necessarily represent the view of the U.S. Department of Energy or the United States.

Sandia National Laboratories is a multi-mission laboratory managed and operated by National Technology and Engineering Solutions of Sandia, LLC, a wholly owned subsidiary of Honeywell International, Inc., for the U.S. Department of Energy's National Nuclear Security Administration under contract DE-NA-0003525.

## REFERENCES

- [1] C. B. Jones, A. Summers and M. J. Reno, "Machine Learning Embedded in Distribution Network Relays to Classify and Locate Faults," 2021 IEEE Power & Energy Society Innovative Smart Grid Technologies Conference (ISGT), 2021, pp. 1-5, doi: 10.1109/ISGT49243.2021.9372247.
- [2] V. Gurevich, Electric Relays: Principles and Applications. CRC Press, Oct. 2018, google-Books-ID: mW3LBQAAQBAL.
- [3] M. J. Reno, S. Brahma, A. Bidram, and M. E. Ropp, "Influence of Inverter-Based Resources on Microgrid Protection: Part 1: Microgrids in Radial Distribution Systems," IEEE Power and Energy Magazine, 2021.
- [4] R. C. Mathews, S. Hossain-McKenzie, and M. J. Reno, "Fault Current Correction Strategies for Effective Fault Location in Inverter-Based Systems," IEEE Photovoltaic Specialists Conference (PVSC), 2019.
- [5] M. Ojaghi and V. Mohammadi, "Use of Clustering to Reduce the Number of Different Setting Groups for Adaptive Coordination of Overcurrent Relays," in IEEE Transactions on Power Delivery, vol. 33, no. 3, pp. 1204-1212, June 2018, doi: 10.1109/TPWRD.2017.2749321.
- [6] M. R. Duff, P. Gupta, D. Prajapati and A. Langseth, "Utility implements communications-assisted special protection and control schemes for distribution substations," 2017 70<sup>th</sup> Annual Conference for Protective Relay Engineers (CPRE), 2017, pp. 1-11, doi: 10.1109/CPRE.2017.8090060.
- [7] A.K Summers, R.C Mathews, T. Patel, M. J. Reno, "Power System Protection Parameter Sensitivity Analysis with Integrated Inverter Based Resources," 2021 IEEE 48th Photovoltaic Specialists Conference (PVSC).
- [8] A. A. Mamun, M. Sohel, N. Mohammad, M. S. Haque Sunny, D. R. Dipta and E. Hossain, "A Comprehensive Review of the Load Forecasting Techniques Using Single and Hybrid Predictive Models," in IEEE Access, vol. 8, pp. 134911-134939, 2020, doi: 10.1109/ACCESS.2020.3010702.
- [9] Y. S. Manjili, R. Vega, and M. M. Jamshidi, "Data-analytic-based adaptive solar energy forecasting framework," IEEE Syst. J., vol. 12, no. 1, pp. 285-296, Mar. 2018, doi: 10.1109/JSYST.2017.2769483.
- [10] S. Opera and A. Bara, "Machine Learning Algorithms for Short-Term Load Forecast in Residential Buildings Using Smart Meters, Sensors and Big Data Solutions," in IEEE Access, vol. 7, pp. 177874-177889, 2019, doi: 10.1109/ACCESS.2019.2958383.
- [11] B. Farsci, M. Amayri, N. Bouguila and U. Eicker, "On Short-Term Load Forecasting Using Machine Learning Techniques and a Novel Parallel Deep LSTM-CNN Approach," in IEEE Access, vol. 9, pp. 31191-31212, 2021, doi: 10.1109/ACCESS.2021.3060290
- [12] <https://mis.ercot.com/public/dashboards>
- [13] Mathews, R.C.; Patel, T.R.; Summers, A.K.; Reno, M.J.; Hossain-McKenzie, S. Per-Phase and 3-Phase Optimal Coordination of Directional Overcurrent Relays Using Genetic Algorithm. *Energies* 2021, 14, 1699. <https://doi.org/10.3390/en14061699>
- [14] Taylor & Benjamin Letham, 2018. "Forecasting at Scale," The American Statistician, Taylor & Francis Journals, vol. 72(1), pages 37-45, January
- [15] B. Reimer, T. Khalili, A. Bidram, M. J. Reno and R. C. Mathews, "Optimal Protection Relay Placement in Microgrids," 2020 IEEE Kansas Power and Energy Conference (KPEC), 2020, pp. 1-6, doi: 10.1109/KPEC47870.2020.9167553